

## Charging performance of quantum batteries in a double-layer environment

Kai Xu,<sup>1,\*</sup> Hong-Guo Li,<sup>1</sup> Zong-Guo Li,<sup>1</sup> Han-Jie Zhu,<sup>2,†</sup> Guo-Feng Zhang<sup>3,‡</sup> and Wu-Ming Liu<sup>2,4,5</sup>

<sup>1</sup>*School of Science, Tianjin University of Technology, Tianjin 300384, China*

<sup>2</sup>*Beijing National Laboratory for Condensed Matter Physics, Institute of Physics, Chinese Academy of Sciences, Beijing 100190, China*

<sup>3</sup>*School of Physics, Beihang University, Beijing 100191, China*

<sup>4</sup>*School of Physical Sciences, University of Chinese Academy of Sciences, Beijing 100190, China*

<sup>5</sup>*Songshan Lake Materials Laboratory, Dongguan, Guangdong 523808, China*



(Received 3 April 2022; revised 4 June 2022; accepted 6 July 2022; published 19 July 2022)

In the process of using quantum resources to improve the performance of quantum battery devices, device performance is highly restricted by decoherence due to the influence of the external environment. In particular, the fact that such devices are subject to complex environmental influences in real scenarios should be taken into account. Here, we investigate the performance (i.e., the internal energy, charging power, and ergotropy) of a quantum battery in a double-layer environment, where the first-layer environment is a single-mode cavity and the second-layer environment is a single reservoir. We are surprised to find that the memory effect of the reservoir does not affect the charging performance of a quantum battery; in sharp contrast, the reduction in the coupling between the quantum battery and the first-layer environment can improve the charging performance of a quantum battery. We then extend our discussion to the case where the second-layer environment consists of multiple reservoirs, each consisting of a single-mode cavity dissipated to the Markovian reservoir. It is shown that the charging performance of the quantum battery can be enhanced by increasing the number of cavities in the second-layer environment and the coupling strength between the first-layer environment and the second-layer environment. Our results may be helpful for realizing optimal charging performance of quantum batteries in a complex environment.

DOI: [10.1103/PhysRevA.106.012425](https://doi.org/10.1103/PhysRevA.106.012425)

### I. INTRODUCTION

With the rapid development of quantum technology, using quantum resources to achieve better performance from new equipment compared with traditional equipment is one of the tasks of modern science and technology [1,2]. In this context, the application of quantum resources to the field of quantum batteries has attracted widespread attention [3–10]. Quantum batteries are small quantum systems that can store energy and extract energy [11]. A good quantum battery should have not only large internal energy and charging power but also large ergotropy. To obtain a good quantum battery, researchers have carried out extensive research on how to improve the performance of the quantum battery [12–16].

At first, people studied to improve the charging performance (i.e., internal energy, charging power, and ergotropy) of a closed quantum battery [17–30]. Researchers have shown that the charging performance of a quantum battery can be improved by using quantum resources [26] such as quantum entanglement and quantum coherence. Furthermore, using adiabatic shortcut technology [27], the collective quantum effect [29], and the harmonic drive [30] can also effectively enhance the internal energy and charging power of a closed quantum battery. These studies have inspired research into the charging process of quantum batteries in more practical

situations. In reality, quantum batteries are inevitably affected by the environment [31,32]. Thus, improving the performance of open quantum batteries is an important issue. Recently, many research schemes to improve the charging performance of open quantum batteries have been proposed [33–50]. For example, Seah *et al.* [45] found that in collision quantum batteries, any coherent protocol has a higher charging power than the charging strategy of the noncoherent protocol. In the  $N$ -spin chain-quantum-battery model with nearest-neighbor jumping interaction [34], the maximum energy of the quantum battery can be obtained by a coherent cavity-driving field or a thermal heat bath. Then considering the situation in which the quantum battery and the charger are in the same environment, the authors of [46] found that the energy stored in the battery can be greatly enhanced in the presence of the quantum jump-based feedback control. Moreover, it has been clarified that the memory effect of the environment is beneficial to the charging process of the quantum battery when the interacting quantum battery and the charger are coupled to their respective heat storage environments [47].

The above studies considered the charging process of quantum batteries in a single environment. However, in experiments, quantum systems that implement quantum batteries can face complex environments [51–53]. In quantum dot systems, electron spin not only is strongly influenced by the surrounding nuclear environment but also is weakly influenced by phonons [51,52]. Considering a nitrogen-vacancy center in diamond, the dynamical behavior of the electron spin qubit is affected by  $^{14}\text{N}$  spin environment and

\*kxu19930314@163.com

†hjzhu20@iphy.ac.cn

‡gf1978zhang@buaa.edu.cn

a proximal  $^{13}\text{C}$  nuclear spin environment [53], which in turn are affected by the spin bath. Motivated by these studies, it is necessary and meaningful to consider how to improve the charging performance of quantum batteries in complex environments.

To do so, in this paper, we consider the charging performance of quantum batteries in an experimentally achievable double-layer environment. The double-layer-environment model can be realized by cavity QED [54,55], circuit QED [56,57], and quantum dots [58]. More specifically, in the quantum dot system, the charge (orbital) degrees of freedom play the role of a single-mode cavity, connecting electron spin to a bath, such as charge fluctuation or phonon noise. In cavity QED, in a single-mode cavity it is easy to connect a qubit to a multimode cavity field. Furthermore, cavity QED with superconducting circuits was experimentally achieved in systems in which superconducting qubits are employed as two-level artificial atoms. For a single-mode cavity, a single-mode inductance-capacitance ( $LC$ ) resonator and a multimode coplanar waveguide resonator have been used. Therefore, in realistic physical systems, the double-layer-environment model is feasible. Based on these realistic physical systems, we first consider the case in which the first-layer environment of the quantum battery is a single-mode cavity and the second-layer environment is a single reservoir. We find that the charging performance of the quantum battery can be enhanced by decreasing the coupling strength between the first-layer environment and the second-layer environment. However, we are surprised to find that the charging performance of quantum batteries is unrelated to the memory time of the reservoir environment. We explain this phenomenon by using pseudomode theory. Then since the number of environments and the coupling strength between the environments have an important effect on the charging performance of the quantum battery, we extend our discussion to the case where the second-layer environment facing the quantum battery is composed of  $N$  reservoir environments. We show that the charging performance of the quantum battery can be improved by increasing the number of environments in the second-layer environment and the coupling strength between the first-layer environment and the second-layer environment.

This paper is organized as follows. In Sec. II, the internal energy, charging power, and extractable work of the quantum battery are reviewed. Section III discusses the influence of the memory time of the second-layer environment and the coupling strength between the quantum battery and the first-layer environment on the charging performance of the quantum battery. In Sec. IV, the effect of the number of reservoir environments in the second-layer environment and the coupling strength between the first-layer environment and the second-layer environment on the charging performance of the quantum battery is considered. The conclusions drawn from the present study are given in Sec. V.

## II. QUANTUM BATTERY

The way to obtain high internal energy, charging power, and extractable work from a quantum battery has always been a topic of concern. In this work, we focus on the charging performance of quantum batteries in finite time  $t$ . In this case,

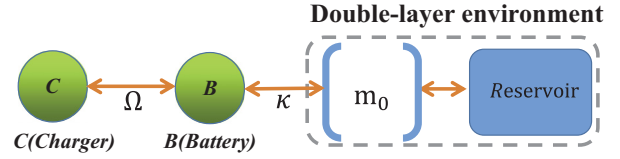


FIG. 1. Schematic diagram of a model of a quantum battery in a double-layer environment. The quantum battery is coupled to a single-mode cavity field  $m_0$ , while the cavity field is coupled to a reservoir  $R$ .

the performances of the charger-battery setup can be studied in terms of the (mean) energy stored in the battery and the corresponding average storing power [29]. The internal energy of the quantum battery at  $t$  is defined as

$$E_B(t) = \text{tr}[H_B \rho_B(t)], \quad (1)$$

where  $\rho_B(t)$  is the reduced density matrix of the quantum battery at time  $t$ . The average charging power of quantum batteries is given by

$$P_B(t) = E_B(t)/t. \quad (2)$$

Then the second law of thermodynamics tells us that not all energy can be extracted from a quantum battery. The amount of energy a quantum battery can output can be measured with ergotropy, i.e.,

$$W_B = \text{Tr}[\rho_B(t)H_B] - \text{Tr}(\sigma_{\rho_B}H_B), \quad (3)$$

where  $\sigma_{\rho_B}$  is the passive counterpart of  $\rho_B(t)$ . Ergotropy represents the maximum energy that can be extracted from a quantum battery at the end of the charging process under cyclic unitary operation. For a two-level quantum battery system, according to the expression for ergotropy, ergotropy can be reduced to a simple form related to the excited-state population of the system. For a specific derivation, refer to Appendix B.

To evaluate the conditions for obtaining the optimal quantum battery, we focus on the maximum internal energy  $E_{\max} = \max_t[E_B(t)] = E_B(t_E)$ , maximum power  $P_{\max} = \max_t[P_B(t)] = P_B(t_E)$ , and maximum ergotropy  $W_{\max} = \max_t[W_B(t)] = W_B(t_E)$ . Here,  $t_E$  corresponds to the time to obtain  $E_{\max}$ ,  $P_{\max}$ , or  $W_{\max}$  of the quantum battery. In the following, we use  $E_B(t)$  ( $E_{\max}$ ),  $P_B(t)$  ( $P_{\max}$ ), and  $W_B$  ( $W_{\max}$ ) to investigate the effect of the two-layer environment on the charging performance of quantum batteries. Larger  $E_B(t)$ ,  $P_B(t)$ , and  $W_B(t)$  are required to obtain the optimal charging performance of quantum batteries.

## III. SINGLE RESERVOIR SERVING AS THE SECOND-LAYER ENVIRONMENT FOR THE QUANTUM BATTERY

We consider a quantum battery in a two-layer environment consisting of the single-mode cavity  $m_0$  and the reservoir  $R$ , as shown in Fig. 1. The single-mode cavity  $m_0$  is the first-layer environment of the quantum battery, and the reservoir  $R$  serves as the second-layer environment of the quantum battery. The total system Hamiltonian is

$$H = H_0 + H_I. \quad (4)$$

Here,  $H_0 = \omega_0 \sigma_+^B \sigma_-^B + \omega_0 \sigma_+^C \sigma_-^C + \omega_0 a^\dagger a + \sum_k \omega_k b_k^\dagger b_k$  is the Hamiltonian of each subsystem (i.e., the terms in  $H_0$  represents the Hamiltonian of the quantum battery, the charger, the single-mode cavity field  $m_0$ , and the reservoir  $R$ , respectively);  $H_I = \Omega(\sigma_+^B \sigma_-^C + \sigma_-^B \sigma_+^C) + \kappa(\sigma_+^B a + \sigma_-^B a^\dagger) + \sum_k g_k (ab_k^\dagger + a^\dagger b_k)$  describes the interactions between the subsystems, where the first term in  $H_I$  represents the interaction Hamiltonian between the quantum battery and the charger and the last two terms in  $H_I$  refer to the interaction Hamiltonian between the quantum battery and the cavity  $m_0$  and the interaction Hamiltonian between the reservoir  $R$  and the cavity  $m_0$ . In the interaction picture, the Hamiltonian  $H$  of the total system can be written as

$$H_{\text{int}} = \Omega(\sigma_+^B \sigma_-^C + \sigma_-^B \sigma_+^C) + \kappa(\sigma_+^B a + \sigma_-^B a^\dagger) + \sum_k g_k (ab_k^\dagger e^{i\Delta_k t} + a^\dagger b_k e^{-i\Delta_k t}), \quad (5)$$

where  $\Delta_k = \omega_k - \omega_0$ ;  $\Omega$  and  $\kappa$  indicate the coupling strength between the quantum charger and the quantum battery and the coupling strength between the quantum battery and the cavity mode  $m_0$ , respectively; and  $g_k$  denotes the coupling of the cavity  $m_0$  with mode  $k$  of the reservoir. Here, we consider  $\kappa \ll \omega_0$  to ensure the validity of the rotational-wave approximation (RWA). Then it is worth mentioning that all interactions considered in this paper are obtained under the RWA; hence, the overall excitation number is conserved.

We assume that the initial state of the total system is  $|\phi(0)\rangle = |eg00_k\rangle_{CBm_0R}$ , that is, the quantum charger  $C$  is initially in the excited state  $|e\rangle_C$ , while the quantum battery  $B$ , cavity field  $m_0$ , and reservoir  $R$  are in the vacuum state. Since the effect of dissipation on the timescale of the charging process is negligible and there is only up to one excitation in the total system, the evolution state of the total system is

$$|\phi(t)\rangle = a(t)|eg00_k\rangle_{CBm_0R} + c_1(t)|ge00_k\rangle_{CBm_0R} + c(t)|gg00_k\rangle_{CBm_0R} + c_2(t)|gg10_k\rangle_{CBm_0R} + \sum_k F_k |gg01_k\rangle_{CBm_0R}. \quad (6)$$

Here,  $|1_k\rangle_R = |0 \cdots 1_k \cdots 0\rangle_R$  means that there is one excitation in the  $k$ th mode of the reservoir  $R$ . According to Schrödinger's equation, the time evolution of the total system in the interaction picture with the Hamiltonian is determined by the following differential equations:

$$\begin{aligned} \dot{a}(t) &= -i\Omega c_1(t), \\ \dot{c}_1(t) &= -i\Omega a(t) + (-i)\kappa c_2(t), \\ \dot{c}_2(t) &= -i\kappa c_1(t) + (-i) \sum_k g_k F_k(t) e^{-it\Delta_k}, \\ \dot{F}_k(t) &= (-i)g_k c_2(t) e^{it\Delta_k}. \end{aligned} \quad (7)$$

Integrating  $\dot{F}_k(t)$  with the initial condition  $F_k(0) = 0$  and inserting the solution into  $\dot{c}_2(t)$ , one obtains the integro-differential equation for the amplitude  $c_2(t)$ :

$$\dot{c}_2(t) = -i\kappa c_1(t) - \int_0^t \sum_k |g_k|^2 c_2(t') e^{-i\Delta_k(t-t')} dt'. \quad (8)$$

$\sum_k |g_k|^2 e^{-i\Delta_k(t-t')}$  can be recognized as the correlation function  $f(t-t')$  of the reservoir  $R$ . Based on the fact that the Lorentzian spectrum can be modeled from the ambient noise sources that a single nitrogen-vacancy (NV) spin faces [59], we assume the reservoir  $R$  has a Lorentzian spectrum  $J(\omega) = \Gamma \lambda^2 / \{2\pi[(\omega - \omega_0)^2 + \lambda^2]\}$ , where  $\tau = \lambda^{-1}$  is the correlation time (memory time) of the reservoir environment and  $\lambda$  and  $\Gamma$  refer to the spectrum width of the Lorentzian spectrum and the cavity mode-reservoir coupling strength, respectively. The correlation function  $f(t-t') = \sum_k |g_k|^2 e^{-i\Delta_k(t-t')} = \Gamma \lambda e^{-\lambda|t-t'|}/2$  can be given. Then the differential equations for  $\dot{a}(t)$ ,  $\dot{c}_1(t)$ , and  $\dot{c}_2(t)$  can be solved by the Laplace transform and the inverse Laplace transform. The reduced density matrix of the quantum battery can be obtained, i.e.,  $\rho_{ee}^B(t) = |c_1(t)|^2$  and  $\rho_{gg}^B(t) = 1 - |c_1(t)|^2$ . It is worth noting that we do not consider the cutoff frequency of the reservoir here. A detailed discussion of the reason is given in Appendix A.

According to Eqs. (1)–(3), the internal energy  $E(t)$ , the charging power  $P(t)$ , and the ergotropy  $W(t)$  can be given by

$$\begin{aligned} E(t) &= \omega_0 |c_1(t)|^2, \\ P(t) &= \omega_0 |c_1(t)|^2/t, \\ W(t) &= \omega_0 [2|c_1(t)|^2 - 1] \Theta[|c_1(t)|^2 - 1/2]. \end{aligned} \quad (9)$$

Here,  $\Theta(x - x_0)$  is the Heaviside function, and for the reason why the Heaviside function is in Eq. (9), refer to Appendix B. We consider the above physical quantities to measure the performance of the quantum battery in units of  $\omega_0$ . The charging dynamics process of the quantum battery  $B$  can be analyzed. Then our goal is to obtain the optimal charging performance of the quantum battery in a double-layer environment.

We first discuss how the parameter  $\lambda$ , which reflects the memory time of the reservoir  $R$  (the larger  $\lambda$  is, the shorter the memory time of the reservoir  $R$  is), and the coupling strength  $\kappa$  between the quantum battery and the cavity field  $m_0$  influence the internal energy  $E_B$  and the charging power  $P_B$  of the quantum battery. In Fig. 2, the changes in  $E_B$  and  $P_B$  with  $\Omega t$  are plotted. We find that  $E_B$  and  $P_B$  decrease monotonically with the increase of  $\kappa/\Omega$ , as shown in Figs. 2(a) and 2(b). This can be understood from the perspective of quantum battery energy dissipation. As the coupling strength  $\kappa$  between the quantum battery and the cavity  $m_0$  increases, the energy in the quantum battery will be dissipated into the environment faster, resulting in a decrease in  $E_B$  and  $P_B$ . Furthermore, the effect of  $\lambda$  on the internal energy  $E_B$  of the quantum battery is also considered in Fig. 2(c). In sharp contrast to previous research [47,48] that the quantum battery is directly coupled to the reservoir, we show that the memory time of the reservoir does not affect the internal energy of the quantum battery in a double-layer environment. This means that the charging performance of the quantum battery in a double-layer environment is not related to the memory time of the reservoir. To obtain the optimal charging performance of the quantum battery, a small coupling strength  $\kappa$  between the cavity  $m_0$  and the quantum battery is required.

To fully understand the impact of the memory time of the reservoir  $R$  and the coupling strength between the quantum battery and the cavity field  $m_0$  on the charging performance

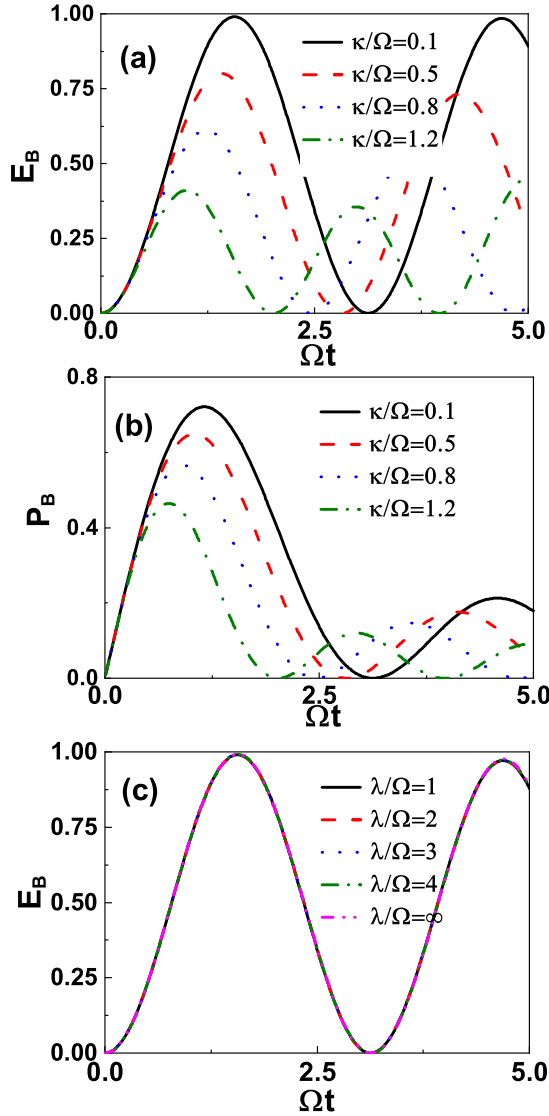


FIG. 2. (a) and (b) The internal energy  $E_B$  and the charging power  $P_B$  of the quantum battery as a function of the dimensionless quantity  $\Omega t$  for different values of the coupling strength  $\kappa/\Omega$  between the quantum battery and the cavity  $m_0$ . (c) The internal energy  $E_B$  of the quantum battery as a function of the dimensionless quantity  $\Omega t$  for different values of  $\lambda/\Omega$ . The parameters are (a) and (b)  $\lambda/\Omega = 0.1$ ,  $\Gamma/\Omega = 1$  and (c)  $\kappa/\Omega = 0.1$ ,  $\Gamma/\Omega = 1$ . The internal energy  $E_B$  and charging power  $P_B$  of a quantum battery are in unit of  $\omega_0$ .

of the quantum battery, the change in the maximum internal energy  $E_{\max}$  with  $\lambda/\Omega$  and  $\kappa/\Omega$  is described in Fig. 3. Consistent with the analysis results in Fig. 2, the maximum internal energy  $E_{\max}$  of the quantum battery in the double-layer environment has nothing to do with the memory time of the reservoir environment. And a smaller  $\kappa$  can result in a larger  $E_{\max}$ . Then, a good quantum battery is supposed to have not only large internal energy and charging power but also large ergotropy. From the expression for ergotropy, the effects of  $\lambda$  and  $\kappa$  on ergotropy are similar to those on  $E_B$ . To verify this more clearly, we plot the variation of the maximum ergotropy  $W_{\max}$  with  $\lambda/\Omega$  and  $\kappa/\Omega$  in Fig. 4. By fixing  $\Gamma/\Omega = 1$ , we find that

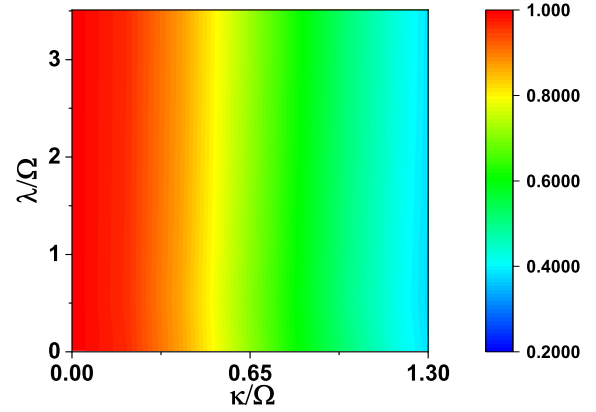


FIG. 3. Maximum internal energy  $E_{\max}$  of the quantum battery as a function of  $\kappa/\Omega$  and  $\lambda/\Omega$ . The parameter is  $\Gamma/\Omega = 1$ . The maximum internal energy  $E_{\max}$  of a quantum battery is in units of  $\omega_0$ .

a critical coupling strength  $\kappa_{\text{cr}}/\Omega = 1.2$  exists between the quantum battery and the cavity field  $m_0$ . The critical coupling strength  $\kappa_{\text{cr}}/\Omega = 1.2$  remains the same only for the case in the analysis. When  $\kappa/\Omega < 1.2$ , the maximum ergotropy  $W_{\max}$  of the quantum battery increases as  $\kappa/\Omega$  decreases. When  $\kappa/\Omega > 1.2$ ,  $W_{\max} = 0$ . Combining the effects of parameters  $\kappa/\Omega$  and  $\lambda/\Omega$  on the maximum internal energy of the quantum battery, a small  $\kappa/\Omega$  is a necessary condition to achieve the optimal charging performance of quantum batteries.

Now, people may be surprised that the memory time of the reservoir environment has no effect on the charging performance of the quantum battery in a double-layer environment. To clarify this problem, we use the pseudomode theory and the energy flow between the quantum battery and the double-layer environment to explain it. In terms of the pseudomode theory [60–64], the pseudomode of the reservoir is an auxiliary variable introduced according to the pole position of the spectral distribution of the reservoir. Each pole is associated with a pseudomode. The coupling between the system of interest and the reservoir can be considered a coherent coupling between the system and the pseudomode, which is dissipated into the Markovian reservoir. By treating the system and pseudomode

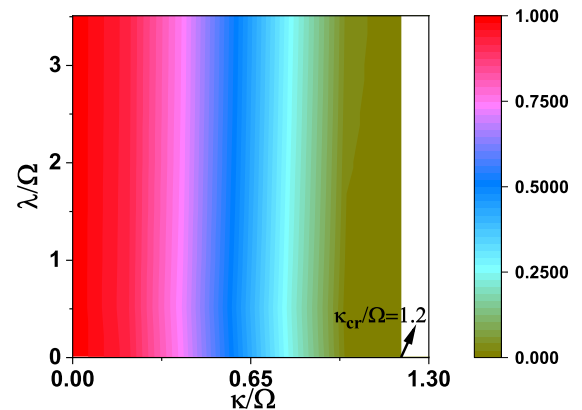


FIG. 4. Maximum ergotropy  $W_{\max}$  of the quantum battery as a function of  $\kappa/\Omega$  and  $\lambda/\Omega$ . The parameter is  $\Gamma/\Omega = 1$ . The maximum ergotropy  $W_{\max}$  of a quantum battery is in units of  $\omega_0$ .

as a larger system, one can obtain the corresponding master equation. For the currently considered quantum battery in a double-layer environment, the density matrix  $\rho(t)$  of the larger system according to the pseudomode theory obeys a master equation with the following form:

$$\dot{\rho}(t) = -i[\hat{H}_0^1, \rho(t)] - \frac{\chi'}{2}[\hat{b}^\dagger \hat{b} \rho(t) - 2\hat{b} \rho(t) \hat{b}^\dagger + \rho(t) \hat{b}^\dagger \hat{b}], \quad (10)$$

where

$$\begin{aligned} H_0^1 = & \omega_0 \sigma_+^B \sigma_-^B + \omega_0 \sigma_+^C \sigma_-^C + \omega_0 a^\dagger a + \omega_0 b^\dagger b \\ & + \Omega(\sigma_+^B \sigma_-^C + \sigma_-^B \sigma_+^C) + \kappa(\sigma_+^B a + \sigma_-^B a^\dagger) \\ & + \eta(ab^\dagger + a^\dagger b), \end{aligned} \quad (11)$$

where  $b^\dagger$  ( $b$ ) is the creation (annihilation) operator of the pseudomode and  $\eta = \sqrt{\Gamma\lambda/2}$  is the coupling strength between the cavity  $m_0$  and the pseudomode, whose dissipation rate is  $\chi' = 2\lambda$ , which satisfies  $\chi' \ll \omega_0$ . Then we define that  $C_1(t)$ ,  $A(t)$ ,  $C_2(t)$ , and  $C_3(t)$  correspond to the probability amplitudes of the quantum battery, charger, cavity field, and pseudomode in their respective excited states, respectively. These probability amplitudes satisfy the following differential equations:  $i\dot{A}(t) = \omega_0 A(t) + \Omega C_1(t)$ ,  $i\dot{C}_1(t) = \omega_0 C_1(t) + \Omega A(t) + \kappa C_2(t)$ ,  $i\dot{C}_2(t) = \omega_0 C_2(t) + \kappa C_1(t) + \eta C_3(t)$ , and  $i\dot{C}_3(t) = (\omega_0 - i\chi'/2)C_3(t) + \eta C_2(t)$ . A detailed derivation can be found in Appendix C.

To evaluate the energy flow between the quantum battery and the overall environment which contains the cavity mode  $m_0$  and the pseudomode, we use the compensation rate  $M(t)$  for the population change in the cavity field and the pseudomode to witness the energy flow to the quantum battery, i.e.,

$$M(t) \equiv d \sum_{n=2}^3 |C_n(t)|^2 / dt + \chi' |C_3(t)|^2, \quad (12)$$

where  $|C_2(t)|^2$  and  $|C_3(t)|^2$  are the excited-state populations of the cavity field mode  $m_0$  and pseudomode, respectively. If the cavity field mode  $m_0$  and pseudomode populations are reduced ( $d[|C_2(t)|^2 + |C_3(t)|^2] / dt < 0$ ) and that reduction cannot be compensated for by the decay to the reservoir due to the term  $\chi' |C_3(t)|^2$ ,  $M(t) < 0$  will occur. Physically, this implies that the energy of the total environment (i.e., mode  $m_0$  and the populated pseudomode) is transferred to the quantum battery, thus leading to the improvement of the charging performance of the quantum battery. In Fig. 5, we plot the witness  $M(t)$  as a function of  $\Omega t$  for different  $\lambda/\Omega$ . It is valuable to point out that no matter how we control  $\lambda/\Omega$ ,  $M(t)$  will transition from  $M(t) > 0$  to  $M(t) < 0$  at the same moment. This means that no matter how the memory time of the reservoir environment  $R$  is manipulated, the energy flow from the cavity  $m_0$  to the quantum battery will appear at the same time, resulting in the quantum battery charging performance being independent of the memory-time changes. Therefore, in our double-layer environment setting, the fundamental reason why the memory time of the reservoir environment has no influence on the charging performance of the quantum battery is that the moment when energy begins to flow from the cavity field  $m_0$  to the quantum battery has no relationship to  $\lambda$ .

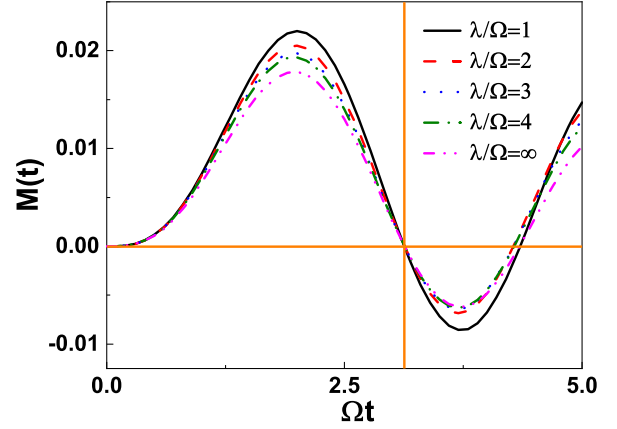


FIG. 5. The witness  $M(t)$  as a function of the dimensionless quantity  $\Omega t$  for different values of  $\lambda/\Omega$ . The parameters are  $\Gamma/\Omega = 1$ ,  $\kappa/\Omega = 0.1$ . Both axes are dimensionless.

#### IV. A NUMBER OF RESERVOIRS SERVING AS THE SECOND-LAYER ENVIRONMENT FOR THE QUANTUM BATTERY

In the previous section, we considered the case where the second-layer environment faced by the quantum battery is only a single reservoir. In this section, we expand the single-reservoir environment to  $N$ -reservoir environments to explore the influence of the number of reservoir environments in the second-layer environment and the coupling strength between the first-layer environment and the second-layer environment on the charging performance of the quantum battery. Here, we model the reservoir environments as bosonic modes that decay to the Markovian reservoir with a decay rate  $\Gamma'$ , as shown in Fig. 6. The Hamiltonian of the total system can be written as  $H = H_0^2 + H_I^2$ , i.e.,

$$\begin{aligned} H_0^2 = & \omega_0 \sigma_+^B \sigma_-^B + \omega_0 \sigma_+^C \sigma_-^C + \omega_0 a^\dagger a + \sum_n \omega_0 d_n^\dagger d_n, \\ H_I^2 = & \Omega(\sigma_+^B \sigma_-^C + \sigma_-^B \sigma_+^C) + \kappa(\sigma_+^B a + \sigma_-^B a^\dagger) \\ & + \sum_n \gamma_n (a d_n^\dagger + a^\dagger d_n), \end{aligned} \quad (13)$$

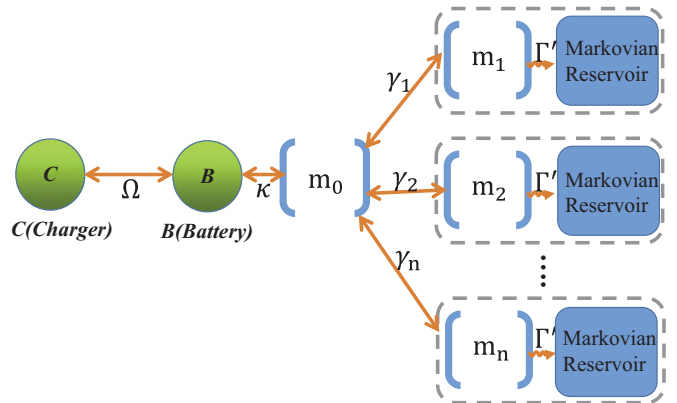


FIG. 6. Schematic diagram of a model of the quantum battery in a double-layer environment. The quantum battery is coupled to a single-mode cavity field  $m_0$ , while the cavity field is coupled to  $N$  reservoir environments.

where  $d_n^\dagger$  ( $d_n$ ) is the creation (annihilation) operator of mode  $m_n$  ( $n = 1, 2, \dots, N$ ). Here, we consider  $\kappa \ll \omega_0$  and  $\gamma_n \ll \omega_0$  to satisfy the condition of the RWA. Then under the Born-Markovian approximation and the RWA ( $\Gamma' \ll \omega_0$ ), the master equation satisfied by the total system can be written as

$$\begin{aligned} \frac{d\rho}{dt} = & -i[H, \rho] - \frac{\Gamma'}{2}(a^\dagger a \rho - 2a\rho a^\dagger + \rho a^\dagger a) \\ & - \sum_{n=1}^N \frac{\Gamma'_n}{2}(d_n^\dagger d_n \rho - 2d_n \rho d_n^\dagger + \rho d_n^\dagger d_n). \end{aligned} \quad (14)$$

We assume that the quantum charger is in the excited state  $|1\rangle_C$  and the quantum battery and other modes are in the vacuum state  $|0\rangle_B|000\dots 0\rangle_{m_0\dots m_n}$ , i.e.,  $\rho(0) = |10\dots 0\rangle\langle 10\dots 0|$ . Since the total system has at most one excitation, the evolution state of the total system at any time can be written as  $\rho(t) = [1 - p(t)]|\psi(t)\rangle\langle\psi(t)| + p(t)|00\dots 0\rangle\langle 00\dots 0|$ , where  $0 \leq p(t) \leq 1$ , and  $|\psi(t)\rangle = g(t)|10\dots 0\rangle + u(t)|01\dots 0\rangle + l_0(t)|001\dots 0\rangle + \dots + l_n(t)|000\dots 1\rangle$ . Then the probability amplitudes  $G(t) = \sqrt{1 - p(t)}g(t)$ ,  $U(t) = \sqrt{1 - p(t)}u(t), \dots, L_n(t) = \sqrt{1 - p(t)}l_n(t)$  of the un-normalized state vector  $|\psi(t)\rangle = \sqrt{1 - p(t)}|\psi(t)\rangle$  are connected to the master equation in Eq. (14). Here,  $G(t)$ ,  $U(t)$ , and  $L_n(t)$  respectively correspond to the probability amplitudes of the excited-state population for the quantum charger, quantum battery, and cavity field mode  $m_n$ . Substituting  $\rho(t) = |\psi(t)\rangle\langle\psi(t)| + p(t)|00\dots 0\rangle\langle 00\dots 0|$  into Eq. (14), we can obtain the following differential equation:

$$\begin{aligned} i\dot{G}(t) &= \omega_0 G(t) + \Omega U(t), \\ i\dot{U}(t) &= \omega_0 U(t) + \Omega G(t) + \kappa L_0(t), \\ i\dot{L}_0(t) &= (\omega_0 - i\Gamma'/2)L_0(t) + \kappa U(t) + \sum_{n=1}^N \gamma_n L_n(t), \\ i\dot{L}_n(t) &= (\omega_0 - i\Gamma'/2)L_n(t) + \gamma_n L_0(t). \end{aligned} \quad (15)$$

By numerically solving the above differential equation, the reduced density matrix of the quantum battery can be obtained. Then according to Eqs. (1)–(3), the internal energy of the quantum battery  $E_B(t)$ , the charging power  $P_B(t)$ , and the ergotropy  $W_B(t)$  can be obtained as

$$\begin{aligned} E_B(t) &= \omega_0 |U(t)|^2, \\ P_B(t) &= \omega_0 |U(t)|^2/t, \\ W_B(t) &= \omega_0 [2|U(t)|^2 - 1]\Theta[|U(t)|^2 - 1/2]. \end{aligned} \quad (16)$$

The above physical quantities are in units of  $\omega_0$ . In the following, we can analyze the impact of the number of cavity modes in the second-layer environments and the coupling strength between the first-layer environment  $m_0$  and the second-layer environment  $m_n$  on the charging performance of the quantum battery.

We first consider the influence of the number of dissipative cavities in the second-layer environment on the internal energy and charging power of the quantum battery, as shown in Figs. 7(a) and 7(b). Since the coupling strength between different cavity modes can be adjusted to the same value in the circuit quantum electrodynamics experimental system

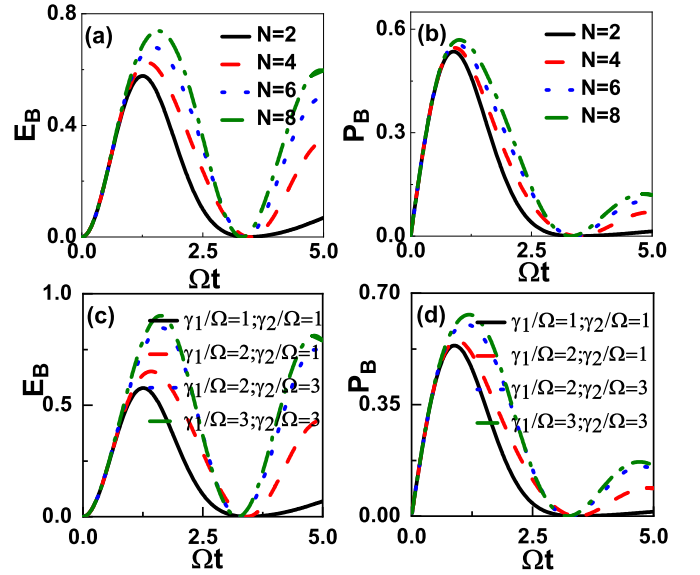


FIG. 7. (a) and (b) The internal energy  $E_B$  and the charging power  $P_B$  of the quantum battery as a function of the dimensionless quantity  $\Omega t$  for different values of the number  $N$  of dissipative cavities. (c) and (d) The internal energy  $E_B$  and the charging power  $P_B$  of the quantum battery as a function of the dimensionless quantity  $\Omega t$  for different values of the coupling strength  $\gamma_n/\Omega$  between cavities  $m_0$  and  $m_n$ . The parameters are (a) and (b)  $\gamma_1/\Omega = \kappa/\Omega = \Gamma'/\Omega = 1$  and (c) and (d)  $N = 2, \kappa/\Omega = \Gamma'/\Omega = 1$ . The internal energy  $E_B$  and charging power  $P_B$  of a quantum battery are in units of  $\omega_0$ .

[65,66], we assume that cavity modes  $m_0$  and  $m_n$  have the same coupling strength (i.e.,  $\gamma_n/\Omega = 1$ ). We find that  $E_B$  and  $P_B$  increase with the increase in the number of lossy cavities, which means that the increase in the number of dissipative cavities in the second-layer environment is conducive to improving the charging performance of the quantum battery. The effect of the coupling strength  $\gamma_n/\Omega$  between modes  $m_0$  and  $m_n$  on the charging performance of the quantum battery is plotted in Figs. 7(c) and 7(d). It is shown that increasing the coupling strength between the first-layer environment and the second-layer environment can enhance the charging performance of the quantum battery. Therefore, to obtain the optimal quantum battery, larger  $\gamma_n/\Omega$  and larger  $N$  are required to stimulate the larger internal energy and charging power of the quantum battery.

Then, to gain a more comprehensive and intuitive understanding of the influence of  $N$  and  $\gamma/\Omega$  (i.e.,  $\gamma_n/\Omega = \gamma/\Omega$ ) on the maximum internal energy  $E_{\max}$  of quantum batteries, the change in  $E_{\max}$  with  $N$  and  $\gamma/\Omega$  is drawn in Fig. 8. Similar to the analysis in Fig. 7,  $E_{\max}$  increases as  $N$  and  $\gamma/\Omega$  increase. Furthermore, the maximum ergotropy  $W_{\max}$  as a function of  $N$  and  $\gamma/\Omega$  is also considered in Fig. 9. We show that the large number  $N$  of dissipative cavities in the second-layer environment and large coupling strength  $\gamma/\Omega$  between the first-layer environment and the second-layer environment can excite larger maximum ergotropy  $W_{\max}$ . Therefore, when considering a quantum battery in a double-layer environment, the optimal charging performance of the quantum battery can be achieved by increasing the number of cavities in the second-

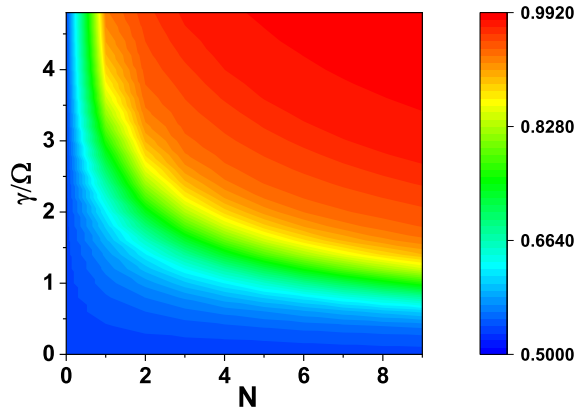


FIG. 8. Maximum internal energy  $E_{\max}$  of the quantum battery as a function of  $N$  and  $\gamma/\Omega$ . The parameters are  $\kappa/\Omega = \Gamma'/\Omega = 1$ . The maximum internal energy  $E_{\max}$  of a quantum battery is in units of  $\omega_0$ .

layer environment and the coupling strength between the first-layer environment and the second-layer environment.

## V. CONCLUSION

In this paper, we have investigated the charging performance of a quantum battery in a double-layer environment. The single-mode cavity is the first-layer environment of the quantum battery, and a single reservoir environment or multiple reservoir environments serve as the second-layer environment of the quantum battery. Taking the second-layer environment faced by the quantum battery to be a single reservoir  $R$ , we were surprised to find that the charging performance of quantum batteries has nothing to do with the memory time of the reservoir, which is in sharp contrast to previous studies [47,48]. We used the pseudomode theory to explain this phenomenon from the perspective of the moment when the energy begins to flow from the cavity field  $m_0$  to the quantum battery, which does not depend on the memory time of the reservoir. Then we showed that a smaller coupling strength  $\kappa$  between the quantum battery and the first-layer environment is beneficial for the charging process of quantum batteries. Therefore, for a single reservoir environment as the

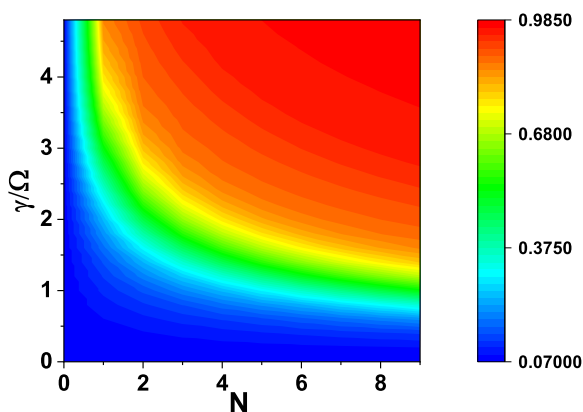


FIG. 9. Maximum ergotropy  $W_{\max}$  of the quantum battery as a function of  $N$  and  $\gamma/\Omega$ . The parameters are  $\kappa/\Omega = \Gamma'/\Omega = 1$ . The maximum ergotropy  $W_{\max}$  of a quantum battery is in units of  $\omega_0$ .

second-layer environment of the quantum battery, to obtain the optimal charging performance of the quantum battery, a small coupling strength  $\kappa$  between the quantum battery and the first-layer environment is required.

Then, we extended our discussion to the case where the second-layer environment faced by a quantum battery is  $N$  reservoir environments. Each reservoir environment was modeled as a case where the bosonic mode decays to the Markovian reservoir. It is worth noting that the charging performance of the quantum battery can be enhanced by increasing the number of cavity field environments in the second-layer environment and the coupling strength  $\gamma$  between the first-layer environment and the second-layer environment. Thus, a large number of dissipative cavities in the second-layer environment and a large coupling strength between the first-layer environment and the second-layer environment are necessary to obtain the optimal charging performance of the quantum battery. These results can provide some theoretical help for realizing the optimal charging process of a quantum battery in a practical complex environment.

## ACKNOWLEDGMENTS

This work was supported by NSFC under Grants No. 12074027, No. 11434015, No. 61227902, No. 61835013, No. 11611530676, and No. KZ201610005011; the National Key R&D Program of China under Grant No. 2016YFA0301500; and SPRPCAS under Grants No. XDB01020300 and No. XDB21030300.

## APPENDIX A: PERFORMANCE OF QUANTUM BATTERIES AT DIFFERENT CUT-OFF FREQUENCIES OF RESERVOIR

To check whether the performance of the quantum battery depends on the cutoff frequency of the reservoir, we consider the reservoir  $R$  to have a Lorentzian spectrum  $J(\omega) = \Gamma\lambda^2 e^{-\omega/\omega_c} / \{2\pi[(\omega - \omega_0)^2 + \lambda^2]\}$ , where  $\omega_c$  is the cutoff frequency of the reservoir. Then the correlation function

$$f(t - t') = \sum_k |g_k|^2 e^{-i\Delta_k(t-t')} = \frac{\Gamma\lambda}{2} e^{-\left(\frac{\omega_0}{\omega_c} - \frac{i\lambda}{\omega_c}\right)(t-t')} e^{-\lambda(t-t')} \quad (\text{A1})$$

can be given. According to Eqs. (7) and (8), the probability amplitudes for  $a(t)$ ,  $c_1(t)$ , and  $c_2(t)$  can be solved by the Laplace transform and the inverse Laplace transform. The reduced density matrix of the quantum battery can be obtained, i.e.,

$$\rho_B = \begin{pmatrix} |c_1(t)|^2 & 0 \\ 0 & 1 - |c_1(t)|^2 \end{pmatrix}. \quad (\text{A2})$$

Then according to Eq. (9), we can analyze the performance of quantum batteries at different cutoff frequencies.

In Fig. 10, we show that the performance of quantum batteries varies with environmental parameters at different cutoff frequencies. More specifically, by fixing  $\omega_c/\Omega = 0.01, 0.1, 1$  in Figs. 10(a)–10(f), we find that the internal energy  $E_B$  and charging power  $P_B$  of quantum batteries decrease with the increase of the coupling strength  $\kappa$  between the quantum battery and the single-mode cavity at different cutoff frequencies. Furthermore, we also show that the internal energy  $E_B$

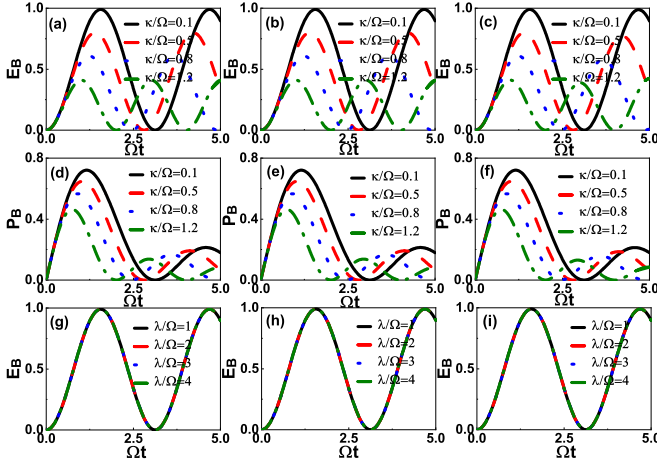


FIG. 10. (a)–(i) The internal energy  $E_B$  and the charging power  $P_B$  of the quantum battery as a function of the dimensionless quantity  $\Omega t$ . The parameters are (a) and (d)  $\omega_c/\Omega = 0.01$ ,  $\lambda/\Omega = 0.1$ ,  $\Gamma/\Omega = 1$ ; (b) and (e)  $\omega_c/\Omega = 0.1$ ,  $\lambda/\Omega = 0.1$ ,  $\Gamma/\Omega = 1$ ; (c) and (f)  $\omega_c/\Omega = 1$ ,  $\lambda/\Omega = 0.1$ ,  $\Gamma/\Omega = 1$ ; (g)  $\omega_c/\Omega = 0.01$ ,  $\kappa/\Omega = 0.1$ ,  $\Gamma/\Omega = 1$ ; (h)  $\omega_c/\Omega = 0.1$ ,  $\kappa/\Omega = 0.1$ ,  $\Gamma/\Omega = 1$ ; and (i)  $\omega_c/\Omega = 1$ ,  $\kappa/\Omega = 0.1$ ,  $\Gamma/\Omega = 1$ . The internal energy  $E_B$  and charging power  $P_B$  of a quantum battery are in units of  $\omega_0$ .

of the quantum battery does not change with the memory time of the reservoir at different cutoff frequencies, as shown in Figs. 10(g)–10(i). This means that in the double-layer environment model we consider, the performance of the quantum battery does not depend on the cutoff frequency of the reservoir.

#### APPENDIX B: THE ERGOTROPY FUNCTIONAL

Let  $\rho$  be the density matrix of a system characterized by the Hamiltonian  $H$ , denoted by the spectral decomposition

$$\rho^{(p)} \equiv \sum r_n |r_n\rangle\langle r_n|, \quad H \equiv \sum e_n |e_n\rangle\langle e_n|, \quad (\text{B1})$$

where  $\{|r_n\rangle\}_n$  and  $\{|e_n\rangle\}_n$  represent the eigenvectors of  $\rho$  and  $H$ , respectively, and  $r_0 \geq r_1 \geq \dots \geq r_n$  and  $e_0 \leq e_1 \leq \dots \leq e_n$  are the associated eigenvalues, which have been properly ordered. The passive counterpart of  $\rho$  is defined as the following density matrix:

$$\sigma^P \equiv \sum r_n |e_n\rangle\langle e_n|. \quad (\text{B2})$$

To find the ergotropy of the quantum battery we can use the reduced density matrix  $\rho_B(t) = |c_1(t)|^2 |e\rangle\langle e|_B + [1 - |c_1(t)|^2] |g\rangle\langle g|_B$  of the quantum battery and Eq. (3); for  $|c_1(t)|^2 \leq 1/2$ , we find that no amount of energy can be extracted from the quantum battery by unitary processes so that  $W_B(t) = 0$  for all  $t$  with  $|c_1(t)|^2 \leq 1/2$ . However, when  $|c_1(t)|^2 > 1/2$ , the ergotropy is given by

$$W_B(t) = \omega_0 [2|c_1(t)|^2 - 1]. \quad (\text{B3})$$

Therefore, by using the Heaviside function  $\Theta(x - x_1)$ , which satisfies  $\Theta(x - x_1) = 0$  for  $x < x_1$ ,  $\Theta(x - x_1) = 1/2$  for  $x = x_1$ , and  $\Theta(x - x_1) = 1$  for  $x > x_1$ , we can write the ergotropy as

$$W_B(t) = \omega_0 [2|c_1(t)|^2 - 1] \Theta[|c_1(t)|^2 - 1/2]. \quad (\text{B4})$$

#### APPENDIX C: THE SYSTEM DYNAMICS

We consider that the quantum charger (C) is initially in the excited state, while the cavity field (F), quantum battery (B), and pseudomode (P) are initially in the vacuum state. Since at most one excitation exists in the total system at any time, the density matrix at any time can be written as

$$\rho(t) = [1 - \lambda(t)] |\psi(t)\rangle\langle\psi(t)| + \lambda(t) |0000\rangle\langle 0000|_{\text{CBFP}}, \quad (\text{C1})$$

where  $0 \leq \lambda(t) \leq 1$ , with  $\lambda(0) = 0$ , and  $|\psi(t)\rangle = a(t)|1000\rangle + c_1(t)|0100\rangle + c_2(t)|0010\rangle + c_3(t)|0001\rangle$ , with  $a(0) = 1$  and  $c_1(0) = c_2(0) = c_3(0) = 0$ . It is convenient to introduce the un-normalized state vector

$$\begin{aligned} |\tilde{\psi}(t)\rangle &\equiv \sqrt{1 - \lambda(t)} |\psi(t)\rangle \\ &= A(t) |1000\rangle + C_1(t) |0100\rangle + C_2(t) |0010\rangle \\ &\quad + C_3(t) |0001\rangle, \end{aligned} \quad (\text{C2})$$

where  $C_1(t)$ ,  $A(t)$ ,  $C_2(t)$ , and  $C_3(t)$  correspond to the probability amplitudes of the quantum battery, charger, cavity field, and pseudomode in their respective excited states, respectively. Then  $\rho(t) = |\tilde{\psi}(t)\rangle\langle\tilde{\psi}(t)| + \lambda(t) |0000\rangle\langle 0000|_{\text{CBFP}}$  can be obtained. Inserting this expression in Eq. (10), the time-dependent amplitudes  $A(t)$ ,  $C_1(t)$ ,  $C_2(t)$ , and  $C_3(t)$  are determined by a set of differential equations as  $i\dot{A}(t) = \omega_0 A(t) + \Omega C_1(t)$ ,  $i\dot{C}_1(t) = \omega_0 C_1(t) + \Omega A(t) + \kappa C_2(t)$ ,  $i\dot{C}_2(t) = \omega_0 C_2(t) + \kappa C_1(t) + \eta C_3(t)$ , and  $i\dot{C}_3(t) = (\omega_0 - i\chi/2) C_3(t) + \eta C_2(t)$ .

[1] M. F. Riedel, D. Binosi, R. Thew, and T. Calarco, *Quantum Sci. Technol.* **2**, 030501 (2017).  
[2] A. Acín, I. Bloch, H. Buhrman, T. Calarco, C. Eichler, J. Eisert, D. Esteve, N. Gisin, S. J. Glaser, F. Jelezko, S. Kuhr, M. Lewenstein, M. F. Riedel, P. O. Schmidt, R. Thew, A. Wallraff, I. Walmsley, and F. K. Wilhelm, *New J. Phys.* **20**, 080201 (2018).  
[3] M. Esposito, U. Harbola, and S. Mukamel, *Rev. Mod. Phys.* **81**, 1665 (2009).  
[4] S. Vinjanampathy and J. Anders, *Contemp. Phys.* **57**, 545 (2016).  
[5] M. N. Bera, A. Riera, M. Lewenstein, Z. B. Khanian, and A. Winter, *Quantum* **3**, 121 (2019).

[6] A. De Pasquale and T. M. Stace, in *Thermodynamics in the Quantum Regime*, edited by F. Binder, L. A. Correa, C. Gogolin, J. Anders, and G. Adesso (Springer, Berlin, 2018).  
[7] M. Carrega, M. Sassetti, and U. Weiss, *Phys. Rev. A* **99**, 062111 (2019).  
[8] G. Benenti, G. Casati, K. Saito, and R. S. Whitney, *Phys. Rep.* **694**, 1 (2017).  
[9] J. Pekola, *Nat. Phys.* **11**, 118 (2015).  
[10] A. Levy and R. Kosloff, *Phys. Rev. Lett.* **108**, 070604 (2012).  
[11] R. Alicki and M. Fannes, *Phys. Rev. E* **87**, 042123 (2013).  
[12] J. Q. Quach and W. J. Munro, *Phys. Rev. Applied* **14**, 024092 (2020).



- [13] F. Pirmoradian and K. Molmer, *Phys. Rev. A* **100**, 043833 (2019).
- [14] Y. Huangfu and J. Jing, *Phys. Rev. E* **104**, 024129 (2021).
- [15] C.-K. Hu, J. Qiu, P. J. P. Souza, J. Yuan, Y. Zhou, L. Zhang, J. Chu, X. Pan, L. Hu, J. Li, Y. Xu, Y. Zhong, S. Liu, F. Yan, D. Tan, R. Bachelard, C. J. Villas-Boas, A. C. Santos, and D. Yu, [arXiv:2108.04298](https://arxiv.org/abs/2108.04298).
- [16] W. J. Lu, J. Chen, L.-M. Kuang, and X. G. Wang, *Phys. Rev. A* **104**, 043706 (2021).
- [17] J.-X. Liu, H.-L. Shi, Y.-H. Shi, X.-H. Wang, and W.-L. Yang, *Phys. Rev. B* **104**, 245418 (2021).
- [18] A. Crescente, M. Carrega, M. Sassetti, and D. Ferraro, *Phys. Rev. B* **102**, 245407 (2020).
- [19] G. M. Andolina, D. Farina, A. Mari, V. Pellegrini, V. Giovannetti, and M. Polini, *Phys. Rev. B* **98**, 205423 (2018).
- [20] J. Chen, L. Y. Zhan, L. Shao, X. Y. Zhang, Y. Y. Zhang, and X. G. Wang, *Ann. Phys. (Berlin, Ger.)* **532**, 1900487 (2020).
- [21] F. Campaioli, F. A. Pollock, F. C. Binder, L. Celeri, J. Goold, S. Vinjanampathy, and K. Modi, *Phys. Rev. Lett.* **118**, 150601 (2017).
- [22] G. M. Andolina, M. Keck, A. Mari, M. Campisi, V. Giovannetti, and M. Polini, *Phys. Rev. Lett.* **122**, 047702 (2019).
- [23] S.-f. Qi, and J. Jing, *Phys. Rev. A* **104**, 032606 (2021).
- [24] T. P. Le, J. Levinsen, K. Modi, M. M. Parish, and F. A. Pollock, *Phys. Rev. A* **97**, 022106 (2018).
- [25] A. C. Santos, A. Saguia, and M. S. Sarandy, *Phys. Rev. E* **101**, 062114 (2020).
- [26] F. H. Kamin, F. T. Tabesh, S. Salimi, and A. C. Santos, *Phys. Rev. E* **102**, 052109 (2020).
- [27] F. Q. Dou, Y.-J. Wang, and J.-A. Sun, *Front. Phys.* **17**, 31503 (2022).
- [28] F. Q. Dou, Y.-Q. Lu, Y.-J. Wang, and J.-A. Sun, *Phys. Rev. B* **105**, 115405 (2022).
- [29] D. Ferraro, M. Campisi, G. M. Andolina, V. Pellegrini, and M. Polini, *Phys. Rev. Lett.* **120**, 117702 (2018).
- [30] Y.-Y. Zhang, T.-R. Yang, L. B. Fu, and X. G. Wang, *Phys. Rev. E* **99**, 052106 (2019).
- [31] H.-P. Breuer and F. Petruccione, *Theory of Open Quantum Systems* (Oxford University Press, New York, 2002).
- [32] M. Nielsen and I. Chuang, *Quantum Computation and Quantum Information* (Cambridge University Press, Cambridge, 2000).
- [33] S. Ghosh, T. Chanda, S. Mal, and A. Sen(De), *Phys. Rev. A* **104**, 032207 (2021).
- [34] F. Zhao, F.-Q. Dou, and Q. Zhao, *Phys. Rev. A* **103**, 033715 (2021).
- [35] F. Zhao, F.-Q. Dou, and Q. Zhao, *Phys. Rev. Research* **4**, 013172 (2022).
- [36] S. Julia-Farre, T. Salamon, A. Riera, M. N. Bera, and M. Lewenstein, *Phys. Rev. Research* **2**, 023113 (2020).
- [37] D. Farina, G. M. Andolina, A. Mari, M. Polini, and V. Giovannetti, *Phys. Rev. B* **99**, 035421 (2019).
- [38] F. Tacchino, T. F. F. Santos, D. Gerace, M. Campisi, and M. F. Santos, *Phys. Rev. E* **102**, 062133 (2020).
- [39] F. Barra, *Phys. Rev. Lett.* **122**, 210601 (2019).
- [40] S.-Y. Bai and J.-H. An, *Phys. Rev. A* **102**, 060201(R) (2020).
- [41] S. Gherardini, F. Campaioli, F. Caruso, and F. C. Binder, *Phys. Rev. Research* **2**, 013095 (2020).
- [42] R. Alicki, *J. Chem. Phys.* **150**, 214110 (2019).
- [43] C. L. Latune, I. Sinayskiy, and F. Petruccione, *Phys. Rev. A* **99**, 052105 (2019).
- [44] K. Xu, H.-J. Zhu, G.-F. Zhang, and W.-M. Liu, *Phys. Rev. E* **104**, 064143 (2021).
- [45] S. Seah, M. Perarnau-Llobet, G. Haack, N. Brunner, and S. Nimmrichter, *Phys. Rev. Lett.* **127**, 100601 (2021).
- [46] Y. Yao and X. Q. Shao, *Phys. Rev. E* **104**, 044116 (2021).
- [47] F. H. Kamin, F. T. Tabesh, S. Salimi, F. Kheirandish, and A. C. Santos, *New J. Phys.* **22**, 083007 (2020).
- [48] F. T. Tabesh, F. H. Kamin, and S. Salimi, *Phys. Rev. A* **102**, 052223 (2020).
- [49] M. Carrega, A. Crescente, D. Ferraro, and M. Sassetti, *New J. Phys.* **22**, 083085 (2020).
- [50] M. T. Mitchison, J. Goold, and J. Prior, *Quantum* **5**, 500 (2021).
- [51] R. Hanson, L. P. Kouwenhoven, J. R. Petta, S. Tarucha, and L. M. K. Vandersypen, *Rev. Mod. Phys.* **79**, 1217 (2007).
- [52] E. A. Chekhovich, M. N. Makhonin, A. I. Tartakovskii, A. Yacoby, H. Bluhm, K. C. Nowack, and L. M. K. Vandersypen, *Nat. Mater.* **12**, 494 (2013).
- [53] Y.-N. Lu, Y.-R. Zhang, G.-Q. Liu, F. Nori, H. Fan, and X.-Y. Pan, *Phys. Rev. Lett.* **124**, 210502 (2020).
- [54] C. J. Hood, T. Lynn, A. Doherty, A. Parkins, and H. Kimble, *Science* **287**, 1447 (2000).
- [55] S. B. Zheng and G. C. Guo, *Phys. Rev. Lett.* **85**, 2392 (2000).
- [56] M. H. Devoret and R. J. Schoelkopf, *Science* **339**, 1169 (2013).
- [57] J. Q. You and F. Nori, *Nature (London)* **474**, 589 (2011).
- [58] G. Burkard, M. J. Gullans, X. Mi, and J. R. Petta, *Nat. Rev. Phys.* **2**, 129 (2020).
- [59] Y. Romach, C. Muller, T. Unden, L. J. Rogers, T. Isoda, K. M. Itoh, M. Markham, A. Stacey, J. Meijer, S. Pezzagna, B. Naydenov, L. P. McGuinness, N. Bar-Gill, and F. Jelezko, *Phys. Rev. Lett.* **114**, 017601 (2015).
- [60] L. Mazzola, S. Maniscalco, J. Piilo, K.-A. Suominen, and B. M. Garraway, *Phys. Rev. A* **80**, 012104 (2009).
- [61] B. M. Garraway, *Phys. Rev. A* **55**, 4636 (1997).
- [62] B. M. Garraway, *Phys. Rev. A* **55**, 2290 (1997).
- [63] B. J. Dalton, S. M. Barnett, and B. M. Garraway, *Phys. Rev. A* **64**, 053813 (2001).
- [64] G. Pleasance, B. M. Garraway, and F. Petruccione, *Phys. Rev. Research* **2**, 043058 (2020).
- [65] P. J. Leek, M. Baur, J. M. Fink, R. Bianchetti, L. Steffen, S. Filipp, and A. Wallraff, *Phys. Rev. Lett.* **104**, 100504 (2010).
- [66] J. M. Fink, M. Goppl, M. Baur, R. Bianchetti, P. J. Leek, A. Blais, and A. Wallraff, *Nature (London)* **454**, 315 (2008).